Experimental Validation of TOA UWB Positioning with Two Receivers Using Known Indoor Features

Jan KIETLINSKI - ZALESKI
School of Engineering
Nagoya University
Nagoya, Japan
jkietlin@katayama.nuee.nagoya-u.ac.jp

Takaya YAMAZATO, Masaaki KATAYAMA
EcoTopia Science Institute
Nagoya University
Nagoya, Japan

Abstract—**Ultra-Wideband is an attractive technology for short range positioning, especially indoors. However, for normal Time of Arrival (ToA) positioning, at least three receivers with unblocked direct path to the transmitter are required. This requirement is not always met. In this work, a novel algorithm for ToA positioning using only two receivers is presented and validated using data from a measurement campaign. Positioning with two receivers is possible by exploiting the knowledge of some of the indoor features, namely positions of big flat reflective surfaces, for example ceiling and walls.**

Keywords-UWB, positioning, TDoA, indoor

I. INTRODUCTION

The main challenge for indoor positioning is the big number of reflections, from walls, furniture and people, that introduce strong fading. The conventional way to combat fading is to increase the bandwidth of the signal, which not only limits fading but also increases time resolution and accuracy of ToA ranging. UWB, with its ultra wide bandwidth, is then a natural choice for high precision indoor positioning. Such positioning has many possible applications, for example in-building goods tracking, workers monitoring or access control[1].

Three Dimensional (3D) Time of Arrival (ToA) Positioning using ranges to three or more receivers is straightforward and has been widely researched [2]. However, when only two receivers are available, two ranges are not enough to find the 3D transmitter position. Conventional approach is to reduce the problem to 2D by assuming height [3]. Approach that, apart from not estimating height, can introduce a significant height-related 2D bias to the results.

In our previous paper [4] we proposed an algorithm for two receiver positioning that uses high time resolution of UWB signals as well as knowledge of reflective surfaces in the environment to estimate a full 3D position.

In this paper we will introduce a new, improved version of the algorithm and we will verify the validity of the algorithm with measurement results.

High time resolution of UWB signals enables us to distinguish different multi-path components (MPCs) in the received signal, which are caused by reflections and diffractions from indoor features. We will use delays of reflected MPCs together with the knowledge of the position of reflective surfaces to help positioning.

The rest of the paper is organized as follows:

We start with a general description of the problem in section II. Next in section III, we define the system elements. We then introduce our own algorithm in section IV dividing it into result circle calculation step in IV-A and ML on-circle position estimation step in IV-B. Then, in section V we introduce our measurement setup. Next, in section VI we present results of the proposed algorithm when used with measurement data. Finally, we draw conclusions in section VII.

II. PROBLEM STATEMENT

In ToA ranging transmitter T and receivers $\mathbf{R} = [R_1, \cdots, R_N]$ are considered to be synchronized. Range from receiver R_N to transmitter T, d_n, can be calculated from signal reception time t_n:

$$\hat{d}_n = \mathrm{C}(t_n - t_0) \qquad n = 1, \ldots, N \tag{1}$$

where C is the speed of light and t_0 is send time.

Next, using calculated $[\hat{d}_1, \cdots, \hat{d}_N]$ a set of quadric equations describing transmitter's position $T := [x_t, y_t, z_t]$ can be formed:

$$\begin{cases} (x_1 - x_t)^2 + (y_1 - y_t)^2 + (z_1 - z_t)^2 = \hat{d}_1^2 \\ \vdots \\ (x_N - x_t)^2 + (y_N - y_t)^2 + (z_N - z_t)^2 = \hat{d}_N^2 \end{cases} \tag{2}$$

where $R_n := [x_n, y_n, z_n]$ is the position of receiver n.

For N>3 a data fusion method, such as Least Squares, would be used.

For N=3 the set could be solved directly.

If N=2, there are only two receivers and the solution of the set is a circle (in a non-degenerate case).

This is not enough information to find a 3D position of the transmitter. The conventional solution is to reduce the problem to 2D by assuming the height coordinate. This approach performs well for applications where transmitter's height is known and nearly constant.

However, if it is not true, it will produce a bias. Since those biases are height-related, they also cannot be reduced by

averaging (in case of a moving tag). To solve this problem, to find the 3D transmitter position, we use information contained in received MPCs.

If it was known which MPCs correspond to reflections from known reflectors, the problem of using MPC delays with the reflector positions for positioning would be trivial. Each extra MPC would be like adding a range measurement to an imaginary receiver, mirror image of the real receiver.

Unfortunately, indoor environment is reflection-rich and finding correct pairings between reflectors and MPCs is hard. A graphic example is presented in Fig. 1.

III. System Model

Consider a system with a mobile UWB transmitter sending impulses that are received by a set of N stationary receivers $\mathbf{R} = [R_1, \cdots, R_N]$. Each receiver is described by its 3D position vector, $R_n := [x_n, y_n, z_n]$. Signal at R_n is often represented in the literature as:

$$r_n(t) = \sum_{k_n=1}^{K_n} \alpha_{k_n} s(t - \tau_{k_n}) + n(t) \tag{3}$$

where K_n is the number of MPCs, α_k and τ_k are the fading coefficient and delay of k_{th} MPC, respectively, $n(t)$ is zero-mean additive white Gaussian noise (AWGN) and $s(t)$ is the transmitted pulse shape. Subscript n defines to which receiver's received signal the parameter applies to.

The transmitter $T := [x_t, y_t, z_t]$ is inside Service Area SA, defined by vector $[x_{\min}, y_{\min}, z_{\min}, x_{\max}, y_{\max}, z_{\max}]$.

$$T \in SA \Leftrightarrow \begin{matrix} x_{\min} \le x_t \le x_{\max} \\ y_{\min} \le y_t \le y_{\max} \\ z_{\min} \le z_t \le z_{\max} \end{matrix} \tag{4}$$

No knowledge about transmitter's position in SA is assumed.

Knowledge of a set of M big, flat reflective surfaces, for example ceiling and walls, is assumed. It is represented as $\mathbf{FR} = [FR_1, \cdots, FR_M]$. Each reflector FR_m is described by roughness $\sigma^2_{FR_m}$ and a 3D surface equation:

$$\begin{matrix} A_m x + B_m y + C_m z + D = 0 \\ \sqrt{A_m^2 + B_m^2 + C_m^2} = 1 \end{matrix} \tag{5}$$

where $[A_m, B_m, C_m, D_m]$ are normalized surface coefficients of reflector FR_m and $[x, y, z]$ are coordinates in 3D space. Roughness $\sigma^2_{FR_m}$ is the assumed added path length variance caused by reflection from FR_m. $\sigma^2_{FR_m}$ models both error in assumed reflector position and irregularities of the reflector. The knowledge of **FR** can be either given a priori, or gained using a calibration step[5].

Mirror image of receiver R_n through flat reflector FR_m will be denoted as R_n^m.

$$R_n^m = R_n - 2(R_n \cdot [A_m\ B_m\ C_m] + D_m) * [A_m\ B_m\ C_m] \tag{6}$$

where $R_n^m := [x_n^m, y_n^m, z_n^m]$. R_n^m will be of use because a FR_m-reflected path between transmitter and receiver R_n can be represented as a direct path between transmitter and R_n^m.

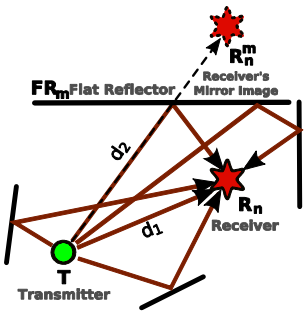

Figure 1. Example - Many reflected MPCs coming to the receiver

In ranging, all receivers R_n can detect not only first, but all distinct MPCs. Result of ranging is a vector of measured MPC arrival times $[\hat{t}_n^1, \cdots, \hat{t}_n^J]$, where $\hat{t}_n^j$ is assumed to have a gaussian error distribution: $\hat{t}_n^j = t_n^j + e_n^j \sim N(0, \sigma_n^{j2})$. Not all MPCs will be detected, so $J_n < K_n$, K_n being MPCs total number.

N vectors of distance estimates $\mathbf{d_n} = [\hat{d}_n^1, \cdots, \hat{d}_n^J]$ are calculated from $[\hat{t}_n^1, \cdots, \hat{t}_n^J]$ using

$$\begin{matrix} \hat{d}_n^1 = \mathrm{C}(\hat{t}_n^1 - t_0) \\ \hat{d}_n^j = d_n^j + e_n^j \sim N(0, \mathrm{C}^2 \sigma_n^{j2}) \end{matrix} \tag{7}$$

There will be a positive bias in $\hat{d}_n^j$ if the corresponding MPC path crossed any obstacle.

We assume that the MPCs corresponding to direct paths are detected, as well as most of MPCs corresponding to the **FR** -reflected paths (i.e. paths reflected by different FR_m). Under those assumptions, the distance of the first incoming MPC, $\hat{d}_n^1$ corresponds to the direct path distance between the transmitter and R_n. Also, the $\mathbf{d_n}$ vector will contain a subset corresponding to **FR** -reflected path distances.

IV. Position Estimation With Two Receivers

A. Result Circle (RC)

If there are only two receivers available ($N = 2$), the solution of (2) in a non-degenerate case will be a circle with one degree of freedom. We assume the transmitter to be near to this result circle (*RC*). *RC*, shown on Fig. 2 can be described parametrically as:

$$\begin{cases} x_t' = r_c \cos(\alpha_t) \\ y_t' = r_c \sin(\alpha_t) \\ z_t' = 0 \end{cases}, \quad T = Q(T') \tag{8}$$

where $T' := [x_t', y_t', z_t']$ are possible transmitter positions in prime base, on XY plane, r_c is result circle's radius, α_t is a free parameter, $T := [x_t, y_t, z_t]$ are possible transmitter positions in real base and $Q(\cdot)$ is a translation plus rotation transform that moves the result circle from prime base to real base. Transmitter position on the *RC* is uniquely described by $r_c \alpha_t$. Transmitter position in real base can be described as $T(r_c \alpha_t)$. Since we assume that $T \in SA$, only $r_c \alpha_t : T(r_c \alpha_t) \in SA$ will be considered.

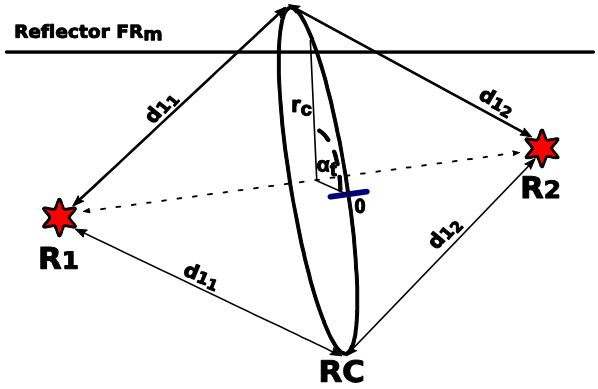

Figure 2. Result Circle with α_t angle noted

B. Position on RC Calculation Algorithm

The second part of the proposed algorithm is to calculate a likelihood profile for all possible $T(r_c\alpha_t)$, based on the knowledge of MPCs and reflection surfaces.

For each receiver/reflector pair $(\mathrm{R_n}, \mathrm{FR_m}) \in \mathbf{R} \times \mathbf{FR}$ we assume a big chance that a MPC range $\hat{d}_n^j \in \mathbf{d_n}$ corresponding to a FR_m-reflected path to R_n was detected. This path can be represented as a direct path to R_n^m, as discussed in Section III. Let us also assume that the error of MPC detection is Gaussian with $\sigma_n^{m2} = \sigma_n^2 + \sigma_{FR_m}^2$, σ_n^2 being range measurement variance (assumed constant for all MPCs), $\sigma_{FR_m}^2$ being reflector's roughness. Then, we can construct a partial likelihood function for possible $T(r_c\alpha_t)$, $L_n^m(\mathbf{d_n}; r_c\alpha_t)$, as follows:

$$L_n^m(\mathbf{d_n}; r_c\alpha_t) = N_{\mathrm{rm}}\left(P_{\mathrm{ndet}} + \sum_{j=0}^{J_n} P_j \mathrm{e}^{-\frac{1}{2}\left(\frac{d(r_c\alpha_t)-d_j^n}{\sigma_n^m}\right)^2}\right) \quad (9)$$

where N_{rm} is a normalization constant, P_{ndet} represents the chance that the correct MPC was not detected, $d(r_c\alpha_t)$ is the distance between R_n^m and $T(r_c\alpha_t)$, d_j^n is the range for j-th MPC in the R_n received signal. P_j is a penalty lowering contributions from early MPCs to offset the tendency of the algorithm to assign high probability near reflector FR_m.

$$P_j = \min\left(\exp\left(-P_{\mathrm{fst}}\left(1 - \frac{d_j^n - d_1^n}{d_{\max}}\right)\right), 1\right) \quad (10)$$

where P_{fst}, first MPC penalty, and $d_{\max}$, maximum penalty length, are algorithm parameters.

Fig. 3 shows the connection between R_n, R_n^m, $d(r_c\alpha_t)$ and $L_n^m(\mathbf{d_n}; r_c\alpha_t)$. Fig. 4 presents a sample $L_n^m(\mathbf{d_n}; r_c\alpha_t)$function.

If the right d_j^n was detected, there should be a $L_n^m(\mathbf{d_n}; r_c\alpha_t)$ maximum near true position of T. In majority of cases however, there will be more than one maximum. If we combine all $L_n^m(\mathbf{d_n}; r_c\alpha_t)$ though, maximums near real position should overlap while other maximums only randomly. If we assume that L_n^m for different n and m are independent, we can calculate the total likelihood function $L(r_c\alpha_t)$ as:

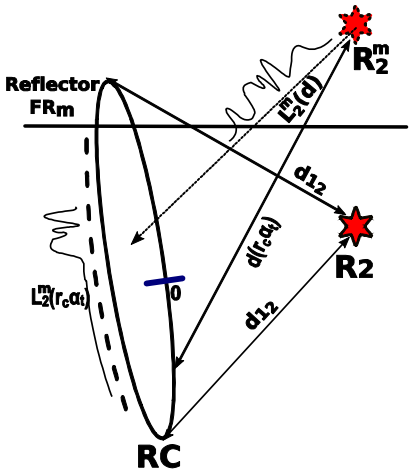

Figure 3. Result Circle with $L_n^m(r_c\alpha_t)$ marked

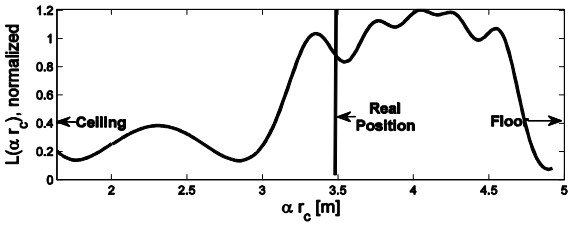

Figure 4. Likelihood function for T_{REF}, 1.5m, R_3-and left wall as reflector.

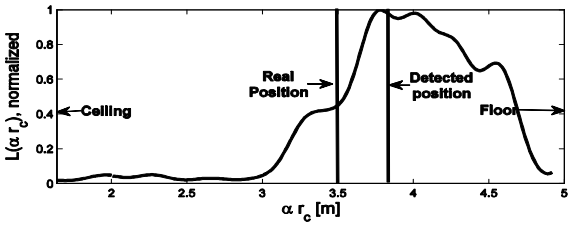

Figure 5. Total likelihood function for T_{REF} and 1.5m

$$L(r_c\alpha_t) = \prod_{n\in[1,N],m\in[1,M]} L_n^m(\mathrm{r_c}\alpha_t) \quad (11)$$

Assumption of the independence of L_n^m is not strictly correct, but the introduced error should be small. Fig.5 shows a sample total likelihood function. Finally, $r_c\alpha_t$ estimate can be found by maximizing likelihood:

$$r_c\alpha_t = \underset{r_c\alpha_t}{\mathrm{argmax}}\left(\sum_{n\in[1,N],m\in[1,M]} \ln(L_n^m(\mathrm{r_c}\alpha_t))\right) \quad (12)$$

The result transmitter position is $T(r_c\alpha_t)$. A flowchart of the complete algorithm is presented in Fig. 6.

V. Measurement Setup

Measurements were performed at Warsaw University of Technology (PW), Department of Electronics and Information Theory (EiTI), in cooperation with Dr. Jerzy Kolakowski, Radiomeasurement Laboratory. The measurement setup schematic is presented on Fig. 7.

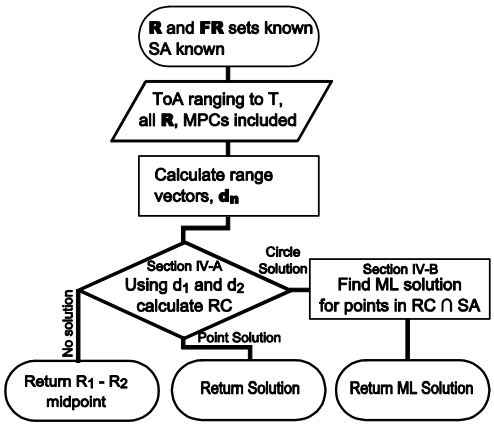

Figure 6. Flowchart of the proposed algorithm

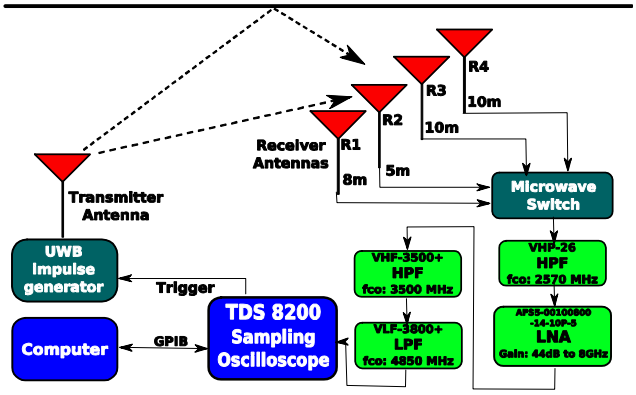

Figure 7. Measurement Setup schematic

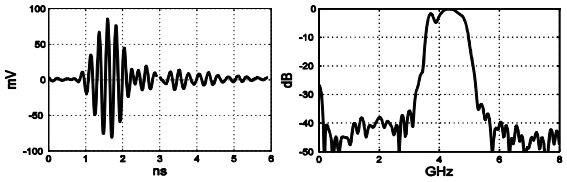

Figure 8. Signal used in measurements

TABLE I.
PARAMETERS USED IN THE PROPOSED ALGORITHM

Parameter	*Value*
P_{ndet}	0.05
P_{fst}	1.25
$d_{\max}$	1.5m
σ_n	0.10m
σ_{FR_1}	0.12m
σ_{FR_2}	0.18m
σ_{FR_3}	0.20m
σ_{FR_4}	0.20m
σ_{FR_5}	0.30

The transmitted signal was designed to roughly correspond to the 3.4-4.8 GHz band. It is shown in Fig. 8. The service area was a classroom, as presented on Fig. 9. Receivers R1, R3 and R4, were used. The considered reflectors were: ceiling, floor, left, right and door walls, in that order. Measurements were

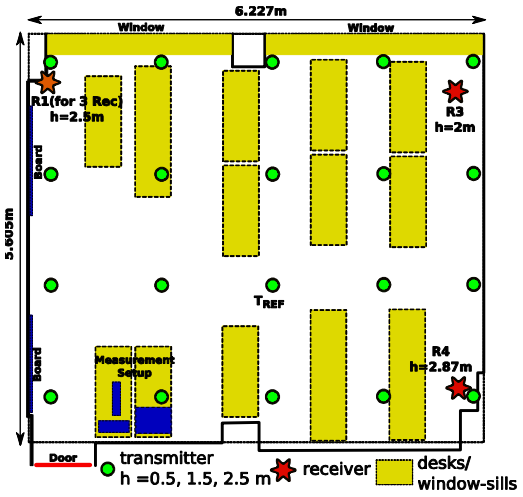

Figure 9. Experiment Layout. Lecture Room S36, EiTI, PW

performed for receivers at heights of 0.5, 1.5 and 2.5m placed at points shown in Fig. 9 for a total of 60 positions. Modified CLEAN algorithm was used for MPC detection in received signals[6]. Used algorithm parameters are presented in table I.

VI. MEASUREMENT RESULTS

The results for different algorithms while using data from the experiment are shown in Figs. 10 and 11. The results are presented as 3D and 2D mean average errors (MAE), averaged over 60 transmitter positions.

Figure 10 shows 3D MAE results for different algorithms, depending on the number of reflectors used. As expected, standard positioning with three receivers produces best results, with MAE of 36cm. This shows that, in practice, using the proposed algorithm cannot fully compensate for losing a third receiver. Standard algorithm for two receiver positioning, Assumed Height, has MAE of 91 cm. Neither of those two algorithms is affected by the number of reflectors because they are not used.

Older Least Squares algorithm presented in [4], is shown to be always worse than Assumed Height algorithm when experimental data is used. LS algorithm was validated only by simulation results, it did not work well with too many closely spaced detected MPCs, situation which is often the case in real life situations. The newer Maximum Likelihood algorithm though, for 3 or more reflectors, is around 25% better than the Assumed Height. This algorithm, apart from giving a better approximation of real likelihood, also includes early MPC penalty, which improves the results significantly.

The performance of the proposed ML and LS algorithms with adding 4th and 5th reflectors. This is because those reflectors are of worse quality than the first three. The fourth reflector is the right wall, situated directly behind the receivers. The reflections from this wall always appear very closely to the first MPC, making them hard to detect. Also, the receiver antennas were positioned with antenna's back towards the back wall, making antenna gain very small. 5th wall is the door wall. As can be seen on Fig. 9, this wall is uneven, with pillar

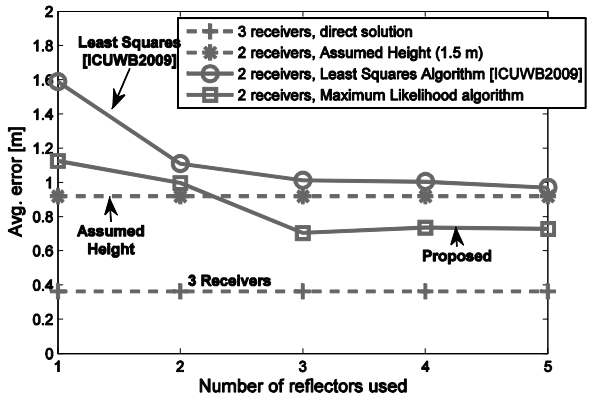

Figure 10. Average 3D positioning error (MAE) for different numbers of known reflectors

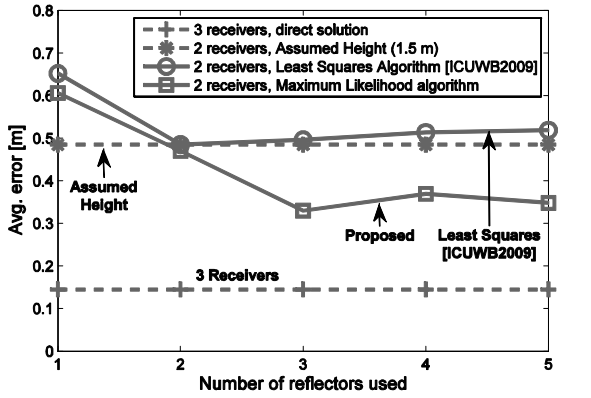

Figure 11. Average 2D positioning error (MAE) for different numbers of known reflectors

interfering and section to the left of the pillar being different depth than section to the right, making a flat reflector a poor approximation of its shape.

In some applications height coordinate of the target is not important. For that reason Fig. 11 shows 2D MAE results, omitting height. The ML algorithm is still better, for 3 or more reflectors, than Assumed Height algorithm. This is because a height error translates directly into a 2D bias. What is surprising is that proposed algorithm's lead is slightly bigger, when compared to 2D. This is because of the contributions of the right wall to the likelihood function, which have symmetry that can lead to big height error but small 2D error.

VII. CONCLUSIONS

In this paper we presented and verified using measurement data a TOA positioning algorithm using 2 receivers and knowledge about indoor reflective surfaces. Measurement results show that in most cases it can determine the transmitter's position with sub-meter accuracy. Comparing to assumed height algorithm it offers better positioning accuracy (for 3 reflectors) and more random error distribution, which is useful in conjunction with position-tracking algorithms.

It is best to be used as a backup scheme in a bigger localization system, for cases when only 2 receivers are reliably in the range of transmitter, because of lower accuracy when compared to 3 receivers case.

[1] Z. Sahinoglu, S. Gezici, and I. Guvenc, Ultra-wideband positioning systems: theoretical limits, ranging algorithms, and protocols, Cambridge Univ Press, 2008

[2] S. Gezici, Z. Tian, G.B. Giannakis, H. Kobayashi, A.F. Molisch, H.V. Poor, and Z. Sahinoglu, "Localization via ultra-wideband radios: a look at positioning aspects for future sensor networks," IEEE Signal Process. Mag., vol.22, no.4, pp.70–84, July 2005.

[3] J. Schroeder, S. Galler, K. Kyamakya, and T. Kaiser,"Three-dimensional indoor localization in non line of sight uwb channels," Proc. IEEE International Conference onUltra-Wideband ICUWB 2007, pp.89–93, 2007.

[4] J. Kietlinski-Zaleski, T. Yamazato, and M. Katayama, "Toa uwb position estimation with two receivers and a set of known reflectors," Proc. IEEE International Conference on Ultra-Wideband ICUWB 2009, pp.376–380, 2009.

[5] T. Deissler and J. Thielecke, "Feature based indoor mapping using a bat-type uwb radar," Proc. IEEE International Conference on Ultra-Wideband ICUWB 2009, pp.475–479, 2009.

[6] K. Siwiak, H. Bertoni, and S.M. Yano, "Relation between multipath and wave propagation attenuation," Electronics Letters, vol.39, no.1, pp.142–143, 9 Jan 2003.

[7] J. Reed, Introduction to ultra wideband communication systems, an, Prentice Hall Press Upper Saddle River, NJ, USA, 2005.